Decoupling limit of diffusion and structural relaxation predicted by a fragility-tunable glassy model

Hairong Qin,[1] Chun-Shing Lee,[2,3] Chi-Hang Lam,[2] and Yongjun Lü[1,*]
[1]*School of Physics, Beijing Institute of Technology, Beijing 100081, China*
[2]*Department of Applied Physics, Hong Kong Polytechnic University, Hong Kong, China*
[3]*Department of Physics, Harbin Institute of Technology, Shenzhen 518055, China*

(Received 5 June 2023; revised 13 August 2023; accepted 8 September 2023; published 18 September 2023)

A full picture of dynamic properties through diverse glasses remains a great challenge in glassy physics. The kinetic fragility is introduced to classify glass-forming liquids and its relevance to glassy properties is expected to outline the family characteristics of glasses. In this paper we propose a distinguishable-particle glassy model with simple pair interactions. This model sensitively tunes the kinetic fragility in an ultrawide range covering real glassy materials. Using the model, we study the decoupling of self-diffusion and structural relaxation time close to the glass transition, and present the fragility dependence of the fractional Stokes-Einstein relation. The results support the existence of a decoupling limit, which corresponds to a possible lower bound of the fractional Stokes-Einstein exponent in very fragile glass-forming liquids. The microscopic mechanism of the fractional Stokes-Einstein relation is verified by using the hopping-dynamics approach associated with single particles.

DOI: 10.1103/PhysRevB.108.104105

I. INTRODUCTION

If liquid is cooled sufficiently fast, it eventually falls out of thermodynamic equilibrium across a narrow temperature range instead of crystallization. In dynamics, the molecular rearrangement is arrested on the laboratory timescale in this process, resulting in the divergence of viscosity and structural relaxation time. In other words, the liquid is quenched into glassy state. On quenching towards the glass transition, supercooled liquids exhibit rich and complex dynamic behaviors, which have attracted wide interests in the past decades. Computer simulations have revealed the existence of spatiotemporal fluctuations of dynamics: some regions are more or less mobile compared to the average within a certain observation time, being called dynamic heterogeneity [1–4]. The dynamically heterogeneous liquid generally exhibits nonexponential relaxation behaviors. For example, recent experimental and numerical studies have unveiled the presence of various secondary relaxations besides the structural relaxation [5–7]. These puzzling relaxations were believed to result from local dynamic behaviors with special spatial arrangements such as cooperative stringlike motions. Another phenomenon in dynamically heterogeneous liquids is the breakdown of the Stokes-Einstein (SE) relation. At high temperatures, self-diffusion coefficient, D, and viscosity, η, are coupled by $D\eta/T = \text{const}$, namely the SE relation. An alternative SE relation is rewritten in terms of the structural relaxation time τ_α as $D\tau_\alpha/T = \text{const}$ corresponding to $\tau_\alpha \propto \eta$. In supercooled liquids this coupling law breaks down. In general, it is found that D^{-1} does not rise as fast as η/T so that $D\eta/T$ increases by 2–3 orders of magnitude as T_g is approached. This decoupling phenomenon is attributed to the existence of dynamic domains with different relaxation timescales responsible for self-diffusion and viscosity. Numerical results have further shown that the coupling is still held just between D and $(\eta/T)^{-\zeta}$ or $(\tau_\alpha/T)^{-\zeta}$, where $0 < \zeta < 1$, being called the fractional SE relation [8–11].

Glass is a large family composed of diverse materials ranging from polymers, colloids, oxides to metals. They are characterized by disordered microstructure in long range and metastable state in energy. The dynamic properties of glass formers largely vary with materials behind the common characteristics. For example, the slowdown of viscosity and relaxation close to the glass transition depends on the type of glass formers. Some liquids, such as tetrahedral liquids (SiO_2 and GeO_2), behave in nearly Arrhenius fashion, and some, such as polymers, show significant deviation from it. Angell has proposed the classification of supercooled liquids based on how much they deviate from the Arrhenius law: the former is called "strong" liquid and the latter is "fragile" liquid [12–14]. The kinetic fragility, which gives a measure of the deviation from the Arrhenius growth, is defined as $m_d = \partial \log(\tau_\alpha)/\partial(T_g/T)|_{T=T_g}$. Among the glassy family, m_d of silica is approximately 20 [13,15], and the values of polymers exceed 200 [13,16]. As an important dynamic index, the fragility provides a characteristic parameter in describing the glassy dynamics [17]. Another example is the fractional SE relation. Although the coupling of relaxation and self-diffusion remains in fractional regime, the exponent ζ associated with the fractional SE relation is not definitely given, and in fact, it varies with materials in the reported literature: for silica, the prototypical low-fragility liquid, $\zeta = 0.89$ [18]; for Cu-Zr melt, the high-fragility liquid, $\zeta = 0.60$ [19]. However, how the fractional SE relation behaves among glasses defined by the kinetic fragility is less clear. An overall dynamic view requires systematic investigations throughout the whole glass family. Clearly, it is a great challenge for both theoretical and experimental researchers.

*Author to whom correspondence should be addressed: yongjunlv@bit.edu.cn

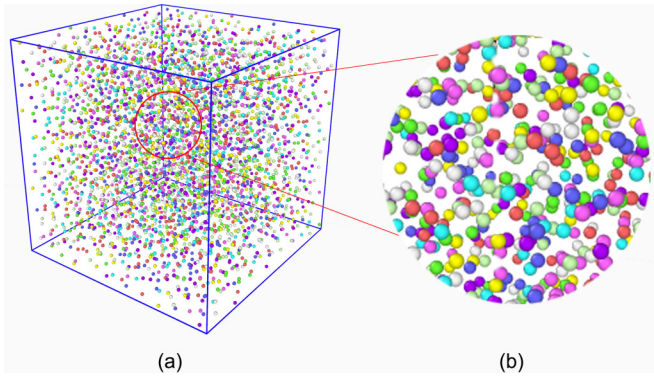

FIG. 1. Configurational diagram of distinguishable-particle glassy model. (a) Global view. (b) Partial enlarged view. Particle color is randomly assigned.

In this work, we propose a distinguishable-particle glassy model (DPGM). This model can tune the kinetic fragility of glass formers via simply controlling a pair-potential parameter. With this model, we simulate the structural model glasses in a wide fragility range of $26 \leqslant m_d \leqslant 343$, which covers most real glassy systems. We show the kinetic-fragility dependence of the fractional SE relation and predict the presence of a lower limit of the relation. We provide a definite microscopic interpretation of the fractional SE relation. The DPGM provides us a promising method to explore thermodynamic and dynamic properties among the glass family.

II. MODEL AND COMPUTATIONAL METHODS

A. Distinguishable-particle glassy model

Inspired by the DPLM proposed in Refs. [20] and [21], we consider a thermodynamic system consisting of N distinguishable particles labeled from 1 to N in 3D. Figure 1 shows the configurational diagram of the distinguishable-particle glass. The N particles are further randomly grouped in two species based on particle size: 80% large (group A) and 20% small (group B) particles. The interaction ϕ_{ij} between any two particles i and j separated by a distance r is given by the Lennard-Jones (LJ) potential,

$$\phi_{ij} = -4V_{ij}\left[\left(\frac{\sigma_{\alpha_i\beta_j}}{r}\right)^{12} - \left(\frac{\sigma_{\alpha_i\beta_j}}{r}\right)^{6}\right], \tag{1}$$

with a distance cutoff of 2.5, where α, $\beta = $ A or B. The depth of potential well V_{ij} for the particle i and j is randomly sampled within $[V_0, V_1] \equiv [-1.25, -0.25]$ from a bicomponent distribution function $g(V_{ij})$ prior to simulations and fixed throughout,

$$g(V_{ij}) = \frac{G_0}{\Delta V} + (1 - G_0)\delta(V_{ij} - V_1), \tag{2}$$

where $\Delta V = V_1 - V_0 = 1$ and δ is the Dirac function. The present range of potential-well depth ($[-1.25, -0.25]$) is determined by referring to other multicomponent systems [22] and after several trials, which is verified to reasonably produce multiple pair-interaction systems that exhibit a wide range of kinetic fragility. In fact, any depth range that satisfies the requirements above is applicable for the model. Different distinguishable-particle families defined by the depth range are scaled by energy. The scaled temperature dependence of dynamic behaviors thus should not show qualitative difference. From Eq. (2), $g(V_{ij})$ consists of a uniform and a delta term, in which the parameter, $G_0 \in [01]$, plays a crucial role in controlling fragility. Actually, G_0 serves as the probabilistic weight of the uniform distribution. For $G_0 = 1$, Eq. (2) reduces to a uniform distribution, producing a strong glass former; for $G_0 = 0$, all the particle pairs have the same LJ energy parameter V_1 and the system is in the high-energy state. The distance parameter σ follows the Kob-Anderson model: $\sigma_{\mathrm{AA}} = 1$, $\sigma_{\mathrm{BB}} = 0.88$, and $\sigma_{\mathrm{AB}} = 0.8$ [23]. This strategy can effectively avoid the occurrence of crystallization and is beneficial for achieving glass transition. The distinguishable-particle model provides a numeric model for some real systems such as polydisperse liquids, in particular, it is analogous to high-entropy alloys in the limit of many atomic species. Different from the void dynamics in crystalline lattice of DPLM, distinguishable-particle glassy model (DPGM) faithfully produces the particle trajectory in a disordered system, which is expected to directly reflect the structural and dynamic characteristics varying with fragility.

B. Molecular dynamics simulations

A distinguishable-particle system consisting of $N = 4000$ particles is prepared. We choose eight G_0 values, $G_0 = 1$, 0.7, 0.4, 0.1, 0.3, 0.01, 0.004, and 0.001, which range from the system with complex particle interactions to the nearly identical-particle system. The initial positions of particles are arranged into the face-centered-cubic structure with the density of 1.69. These systems are quenched from high temperatures and crystallization never occurs in this process. To ensure equilibrium state on cooling, particularly at low temperatures close to the glass transition, we use a two-step simulation procedure: a hybrid Monte Carlo (MC) swap/molecular dynamics (MD) and a conventional MD relaxation. First, a sequence of MC blocks consisting of 10 MC swaps each is carried out, which are separated by several MD blocks consisting of 100 runs each. The total MD steps reach 10^7. Then, a long-time MD relaxation consisting of 4×10^7 MD steps is performed before sampling. All the simulations are performed in the canonical ensemble (NVT) by coupling the system to a Nosé-Hoover thermostat as the glass transition is approached. The periodic boundary conditions are used in the three dimensions and the time step is 0.002 in reduced unit.

III. RESULTS AND DISCUSSION

A. Tunable kinetic fragility

DPGM presents an all-distinguishable-particle system interacted by LJ pair potentials. In this model, each particle is distinguished by the depth of the LJ potential well, V_{ij} which is randomly assigned from a bicomponent distribution function $g(V_{ij})$ [Eq. (2)]. The parameter G_0 ($\in [0,1]$) in $g(V_{ij})$ controls the energy landscape in equilibrium states by weighting the bicomponent distribution. The dynamic behavior of liquids thus is tuned by varying the G_0 value. In analogy to the equilibrium statistic of the distinguishable-particle lattice

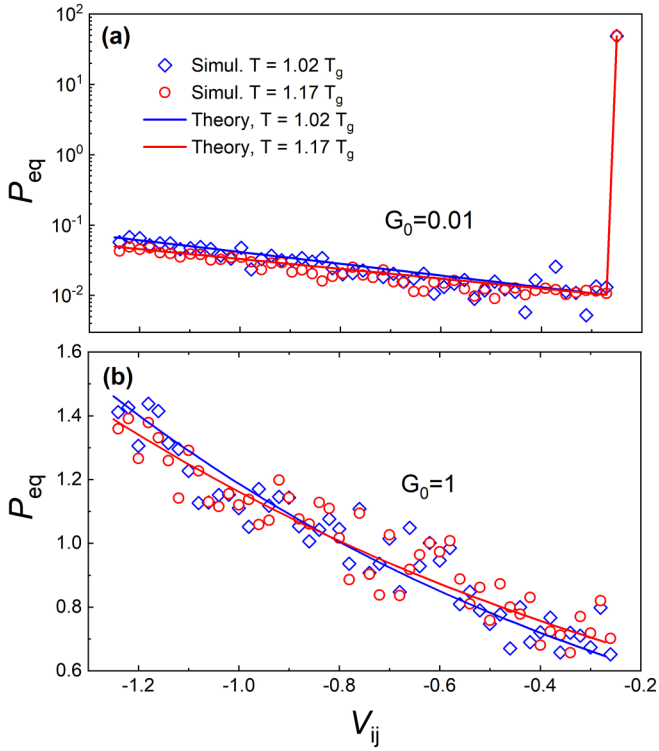

FIG. 2. Distributions of depth of potential well at equilibrium states. (a) $G_0 = 0.01$. (b) $G_0 = 1$. Open circles and diamond symbols are distributions at $T = 1.17\ T_g$ and $1.02\ T_g$ for particle pairs at distance of $1.2\sigma - 1.3\sigma$. Solid lines are analytic results by Eq. (3) in main text.

model [20,21], the particles in DPGM are arranged at equilibrium following the way that the energy depth V_{ij} follows a posterior distribution,

$$p_{\rm eq}(V_{ij}) = \frac{1}{\Lambda} g(V_{ij}) \exp(-V_{ij}/k_B T), \tag{3}$$

where $\Lambda = \int dV g(V) \exp(-V/k_B T)$ is a normalization factor. The particle pairs at a distance of $1.2\sigma - 1.3\sigma$ which is close to the distance at the first peak in the radial distribution function are sampled [24]. We have checked the distributions of V_{ij} on cooling towards glass transition and they agree well with the analytic results predicted by Eq. (3), as shown in Fig. 2, confirming the equilibrium nature in quenching.

We investigate the structural relaxation (α relaxation) by using the self-intermediate scattering function (SISF),

$$F_s(q,t) = \frac{1}{N_0} \sum_{j=1}^{N_0} \langle \exp\{i\mathbf{q} \cdot [\mathbf{r}_j(0) - \mathbf{r}_j(t)]\} \rangle, \tag{4}$$

where N_0 denotes the particle number, $\mathbf{r}_j$ is the position vector of particle j, and the wave number q is determined by the location of the first peak in the structure factor and weakly dependent on temperature. The structural relaxation time, τ_α, is evaluated by fitting SISF to a stretched exponential Kohlrausch-William-Watts function, $\varphi(t) = A \exp[-(t/\tau_\alpha)^\gamma]$, where γ is the stretching exponent. Figure 3(a) shows the dynamic Angell plot, τ_α against T_g/T (the unscaled plot is provided as Fig. S4 in Ref. [24]). Here, we define the glass-transition temperature T_g as the temperature at which $\tau_\alpha = \tau_r = 10^{6.58}$, where the reference relaxation time τ_r is the highest value we can simulate at $G_0 = 0.001$. In fact, in our simulations, the dynamic T_g is approximately consistent with the calorimetric glass-transition temperature, which is determined by the change of the temperature dependence of enthalpy. Thus, the relaxation close to T_g defined in this work faithfully represents the behavior close to the glass transition. The relaxation time monotonically increases with decreasing G_0 at any T_g/T, and the super-Arrhenius behavior is significantly enhanced as G_0 reduces. The temperature dependence of τ_α close to T_g is well described by the Vogel-Fulcher-Tamman (VFT) law, $\tau_\alpha = \tau_0 \exp[BT_0/(T - T_0)]$. Extrapolating the VFT fits up to T_g, we calculate the kinetic fragility that rises with G_0^{-1} following

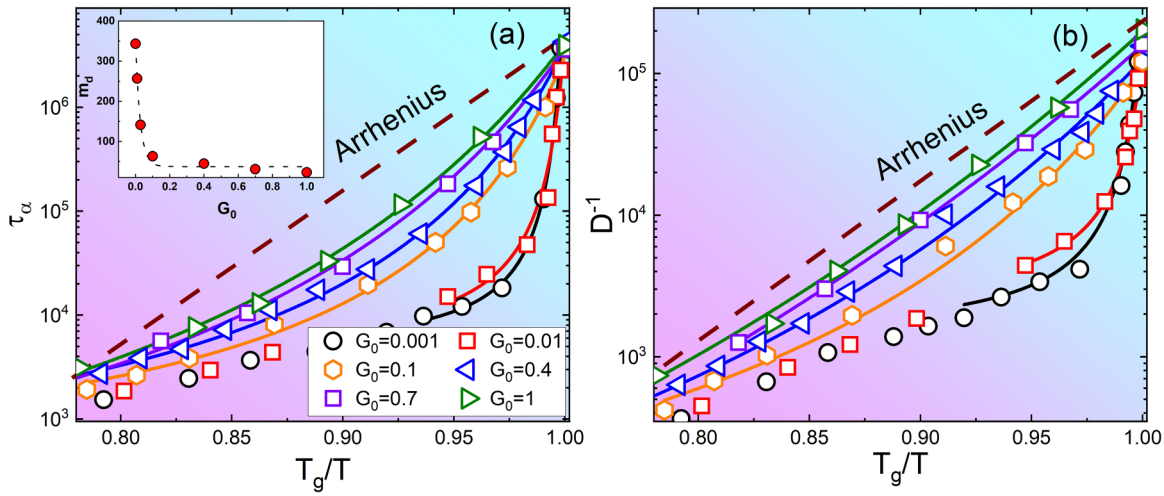

FIG. 3. Angell plots of structural relaxation time and self-diffusion coefficient of DPGM liquids at various G_0. (a) τ_α against T_g/T. Inset shows kinetic fragility defined by structural relaxation time as function of G_0, and dashed line is exponential fit. (b) D^{-1} against T_g/T. Solid lines are Vogel-Fulcher-Tamman (VFT) fits and dashed lines highlight Arrhenius law. Lower-G_0 liquid displays more significant deviation from Arrhenius law, or higher fragility.

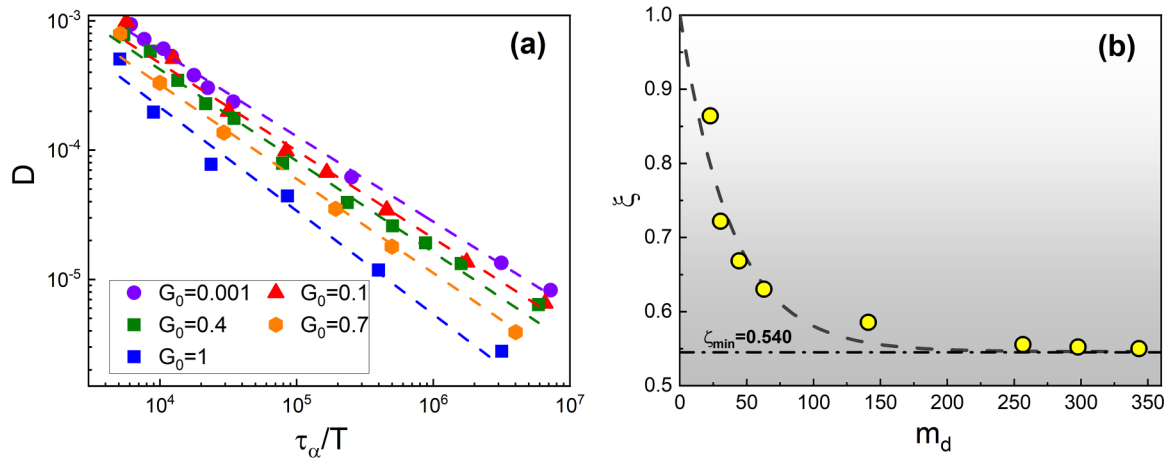

FIG. 4. Fragility dependence of fractional Stokes-Einstein (SE) relation. (a) Plot of D against τ_α/T at various G_0; dashed lines are linear fits. (b) Fractional Stokes-Einstein exponent ζ vs kinetic fragility. Dashed line is fitted result to exponential function.

an exponential law [see inset in Fig. 3(a)]. The smallest and largest values are $m_d = 26$ for $G_0 = 1$ and 343 for $G_0 = 0.001$, respectively. This fragility scope covers most real glassy materials from the prototypical low-fragility liquids to high-fragility ones; in particular, the maximum fragility far exceeds the experimental values of high fragility [25] and even the empirical prediction of the limit of fragility [26,27]. Thus, DPGM exhibits a good ability of tuning fragility in a wide range via simply controlling G_0. From the Angell plot shown in Fig. 3, the lowest-fragility value still slightly deviates from the Arrhenius law, and strictly speaking, the corresponding liquid is only moderately strong. The present DPGM parameters cannot produce the system with the fragility below $m_d = 26$, and here we focus on the dynamic behavior in very fragile systems. In addition, we check the effect of system size on the kinetic fragility. Using a smaller system with $N = 2048$ for $G_0 = 0.1$, the calculated kinetic fragility is approximately $m_d = 61$, which agrees with the result from $N = 4000$ ($m_d = 63$). This excludes finite-size effects on the results presented in this work.

B. Fractional Stokes-Einstein relation in glassy family

Starting from the equilibrium configurations described above, we trace the particle trajectory and then calculate the self-diffusion coefficients based on the mean-squared displacement (MSD), $D = \frac{1}{6N} \lim_{t\to\infty} \sum_{i=1}^{N} \frac{1}{t} \langle |\mathbf{r}_i(t) - \mathbf{r}_i(0)|^2 \rangle$, where $\mathbf{r}_i(t)$ and $\mathbf{r}_i(0)$ are the position vectors of particle i at time t and 0, respectively. The sampling time, t, reaches 3×10^4, which is sufficiently long in diffusion regime (Supplemental Material, Fig. S1) [24]. Figure 3(b) plots D^{-1} against T_g/T, where the glass-transition temperature follows the definition by relaxation time presented above. The super-Arrhenius behavior of D^{-1} is increasingly strengthened with decreasing G_0 analogous to the structural relaxation time, whereas D is not coupled with τ_α/T for all cases of G_0, or the SE relation universally fails. For a clear demonstration, Fig. 4(a) plots D against τ_α/T at various G_0. In the low-temperature regime, the approximately linear relation between them confirms the fractional SE relation instead. Figure 4(b) shows that the exponent $\zeta = 0.860$ for $m_d = 26$ ($G_0 = 1$), which is comparable to the results for some molecular liquids and water [11,28,29]. It rapidly decreases with increasing fragility, and asymptotically approaches a limit in very fragile systems, for example $\zeta = 0.560$ for $m_d = 257$ ($G_0 = 0.01$), $\zeta = 0.552$ for $m_d = 298$ ($G_0 = 0.004$), and $\zeta = 0.550$ for $m_d = 343$ ($G_0 = 0.001$). Given the upper limit of $\zeta = 1$, the fragility dependence of ζ is well fitted to an exponential law $(1 - \zeta_{\min})e^{-\zeta/A_0} + \zeta_{\min}$ function, as the dashed line shown in Fig. 4(b). It predicts a lower limit of the fractional coupling of the SE relation, $\zeta_{\min} \approx 0.540 \pm 0.005$, being independent of fragility.

The tunable fragility in the DPGM could be understood by the temperature variation of excess entropy relative to an ideal distinguishable-particle gas. Our theoretical work has proved that a significant drop of excess entropy occurs on cooling towards T_g in such a distinguishable-particle system [21]. The excess entropy at low T is dominated by the uniform component of $g(V_{ij})$ [see Eq. (3)] that is analogous to the unexcited state in a two-state model [30]. As G_0 decreases, the low-T excess entropy is lowered, resulting in more dramatic drops. It means more sharp reduction in dynamic pathways upon approaching T_g and also more dramatic dynamic slowdown, thus exhibiting higher kinetic fragility.

Violation of the SE relation is a general effect in dynamically heterogeneous glass-forming liquids which manifests the existence of two different measures of relaxation behaviors [2,8–11]. It is commonly believed that the self-diffusion coefficient is dominated by the more mobile particles and the structural relaxation or viscosity gives a measure needed for every particle to move. The two dynamic observables probe different regimes of relaxation time. Enhancing dynamic heterogeneity could broaden the distribution of timescales and is expected to intensify the decoupling between self-diffusion and structural relaxation. On the other hand, in liquids featuring strong dynamic heterogeneity, the structural relaxation is more likely to be dominated by facilitated dynamics rather than thermal activation, displaying strong super-Arrhenius behavior or high fragility. The two aspects qualitatively accounts for why more fragile liquids have smaller SE exponent. From the results shown in Fig. 4, the exponent ζ approaches a lower limit when the liquid becomes very

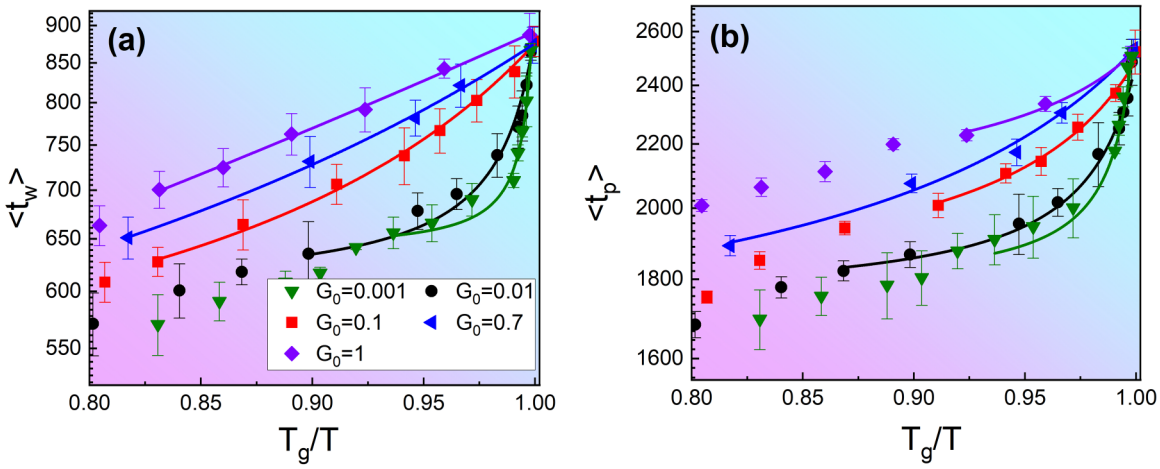

FIG. 5. Hopping dynamics of DPGM liquids at various G_0. (a) Average waiting time $\langle t_w \rangle$ against T_g/T. (b) Average persistence time $\langle t_p \rangle$ against T_g/T. Solid lines are VFT fits to their temperature dependence near T_g.

fragile. It implies a possible existence of a maximum of dynamic heterogeneity.

From reported literature [31,32], we note that the dynamic heterogeneity has been intensively discussed in the 80–20 heterogeneous binary system. The dynamic heterogeneity was thus suggested to stem from the heterogeneous mixture noting that fewer neighbors and wider cage sizes result at a higher mobility. In the present polydisperse system, the dynamic heterogeneity or kinetic fragility is not dominated by the heterogeneous particle size but is indeed determined by the distribution of interactions. The 80–20 particle size used here aims to suppress crystallization and improve glass formation. In fact, we confirm that for a polydisperse system interacting with only a repulsive term, the DPGM has a similar ability of tuning the kinetic fragility by changing the distribution of interactions. This evidence excludes that the present conclusion depends on the 80–20 preset and suggests the DPGM to be generic to the glass family.

From the view of microscopic dynamics, most particles in supercooled liquids are caged within the nearest-neighbor shell to vibrate for a long time, forming immobile regions, until they are activated. The motions of mobile particles are categorized into two types based on their trajectories: random continuous move and hopping motion. The latter is characterized by the sudden displacement jump separated by a long-term cage. As the glass transition is approached, the hopping motion becomes the dominant manner for mobile particles, and plays a crucial role in understanding self-diffusion and relaxation. The hopping motion is further refined into two submotions: the nonreturning hopping motion and the motion that particles hop back to their initial positions, namely the returning hop. The numerical results have shown that the irreversible hopping is responsible for the self-diffusion process [33–37]; the self-diffusion coefficient is measured accurately by $D = \langle l^2 \rangle / 6 \langle t_w \rangle$ at not too low temperatures, where l is the hopping distance and t_w is waiting time between two consecutive nonreturning hops of a particle. Another characteristic time is the waiting time to hop for the first time, also called the persistence time t_p. It has been suggested that the persistence time is related to the structural relaxation [35–39].

We reexamine the contribution of the refined hopping motions to self-diffusion and relaxation. To effectively identify a hopping event, the time-coarse graining of particle positions is performed by $\bar{\mathbf{r}}_i(t) = \frac{1}{\Delta t} \int_0^{\Delta t} \mathbf{r}_i(t + t')dt'$. A hopping event is identified if the moving distance between the two neighboring time-coarse grained positions is larger than a distance threshold. In general, the Debye-Waller factor of liquids is proposed as the characteristic length scale of the rattling motion in cage, which is approximated by the MSD corresponding to the inflection point in the log[MSD]–log T curves, $\langle u^2 \rangle$ that is dependent of temperature (Fig. S1) [24,40]. Here, we adopt the value of $3\langle u^2 \rangle$ as the distance threshold in identifying a hop event. The threshold value increases with temperature and ranges from 0.48 to 0.80 (see Table S1 in Ref. [24]), which is close to the value 0.54 corresponding to the first minimum of the van Hove correlation function adopted in previous studies [41].

After the first hop, the subsequent hop is defined as the returning hop if the particle hops back within a distance of 0.15σ from its original position. If the particle further moves elsewhere beyond a distance of 0.3σ in its second hop, it is defined as the nonreturning hop. Here, the waiting time t_w refers to the time interval between two consecutive nonreturning hops; the persistence time is defined without posterior conditions, namely, it does not require whether the second hop occurs in an observation time window and whether the second hop is the nonreturning or the returning. In general, the hopping dynamics of a single particle is described as a continuous-time random walk. The waiting time, persistent time, and hopping distance are random variables. The average waiting time $\langle t_w \rangle$ and the average persistence time $\langle t_p \rangle$ thus are given by the probability-density functions, $\psi_w(t_w)$ and $\psi_p(t_p)$ as $\langle t_w \rangle = \int_0^\infty t_w \psi(t_w) dt_w$ and $\langle t_p \rangle = \int_0^\infty t_p \psi(t_p) dt_p$, respectively [24]. We would give a microscopic explanation on the fractional SE relation dependent on kinetic fragility based on the hopping dynamics of single particles.

Figure 5(a) shows the Arrhenius plot of the average waiting time $\langle t_w \rangle$ of DPGM glass-forming liquids upon approaching T_g at various G_0. This plot much resembles the Angell plot:

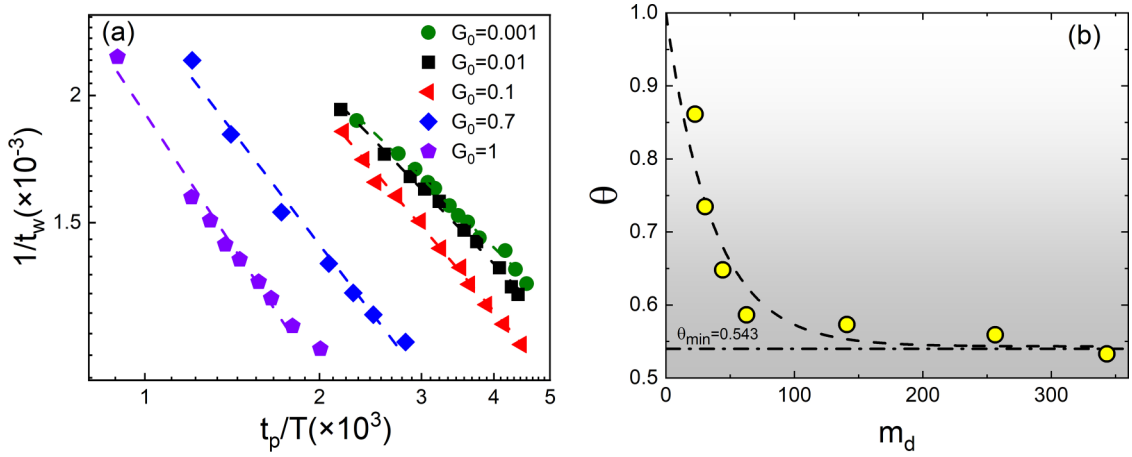

FIG. 6. Interpretation of fractional SE relation in hopping dynamics. (a) Logarithm plot of $1/\langle t_w\rangle$ against $\langle t_p\rangle/T$, and dashed lines are linear fits. (b) Exponent θ associated with fractional coupling between $1/\langle t_w\rangle$ and $\langle t_p\rangle$ vs kinetic fragility. Dashed line is result fitted to exponential function.

more pronounced super-Arrhenius behavior is found in more fragile (lower G_0) liquids. In a microscopic view, in glasses or supercooled melts most particles are caged within their neighbors in a long-time term except few hopping events. The self-diffusion coefficient is actually dominated by successive hopping process, and thus $\langle t_w\rangle$ provides a measure of the timescale of diffusion. The similar non-Arrhenius behavior dependent on fragility is also found in $\langle t_p\rangle$: the more fragile the liquid is, the more pronounced deviation $\langle t_p\rangle$ shows as the glass transition is approached, as shown in Fig. 5(b). If $\langle t_p\rangle$ measures the timescale of structural relaxation, there should be a coupling relation between $\langle t_w\rangle$ and $\langle t_p\rangle$ similar to the fractional SE relation. We plot $1/\langle t_w\rangle$ versus $\langle t_p\rangle/T$ in Fig. 6(a), ranging from $G_0 = 0.001$ to 1. The linear relations are held in all cases and the slopes decrease with increasing fragility. It supports that there exists the coupling between $1/\langle t_w\rangle$ and $(\langle t_p\rangle/T)^\theta$ among the DPGM glassy family. Similar to the fragility dependence of ζ, the exponent θ also shows a lower bound with increasing fragility, as shown in Fig. 6(b). Figure 7 compares the exponent θ with the exponent ζ of the fractional SE relation, showing a good coincidence between them. Therefore, $1/\langle t_w\rangle$ and $\langle t_p\rangle$ provide a definite microscopic picture of the fractional coupling between self-diffusion coefficient and structural relaxation time. It manifests that the first hops take more time to be activated compared to successive hops, and they measure different dynamic regimes. The persistence time rises more sharply during quenching towards T_g when the liquid becomes more fragile, which leads to smaller exponent for the fractional coupling.

Understanding the hopping dynamics varying with fragility is of importance to interpret the effect of fragility on the fractional SE relation. Several theoretical and simulation studies have attempted to relate the spatiotemporal morphologies of hopping dynamics to complex relaxation phenomena in glasses [7,42–48]. In the system with facilitated dynamics, immobile (caged) regions tend to be activated by mobile (hopping) regions. The persistence time associated with the first hopping is largely determined by how much the immobile regions can be facilitated by hops. It is evident that this process is related to the interfacial area between immobile and mobile regions; the more heterogeneously the mobile regions distribute, the longer time it takes to relax immobile regions. We calculate the probability-density distribution of hopping events at various G_0. Figure 8 presents the three slices of probability-density distribution along the z axis at $T = 1.02\ T_g$ and at $G_0 = 1$, 0.01, and 0.001, respectively. These slices are colored at the same scale. In a whole, the hopping is significantly suppressed with decreasing fragility irrespective of the first or the successive hops, manifesting the universal slowdown of glassy dynamics. It is consistent with the slower diffusion and structural relaxation found in less-fragile liquids at given scaled temperatures. A remarkable change is that the dynamic heterogeneity is

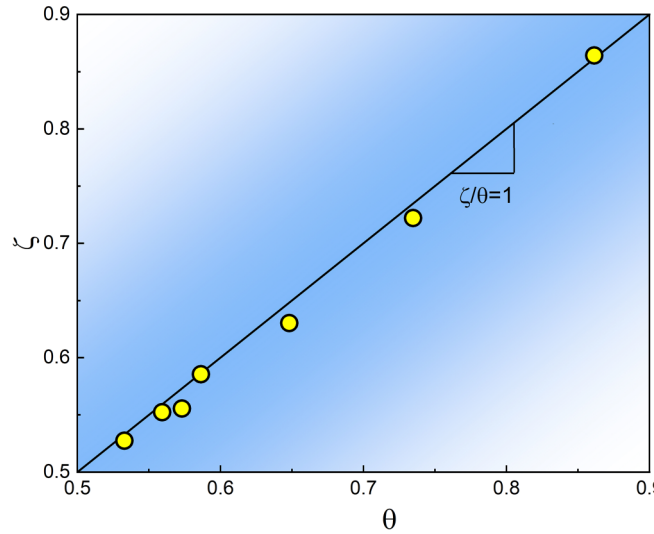

FIG. 7. Exponent θ vs fractional SE exponent ζ. Comparison shows good coincidence between θ and ζ, indicating microscopic mechanism responsible for fractional SE relation.

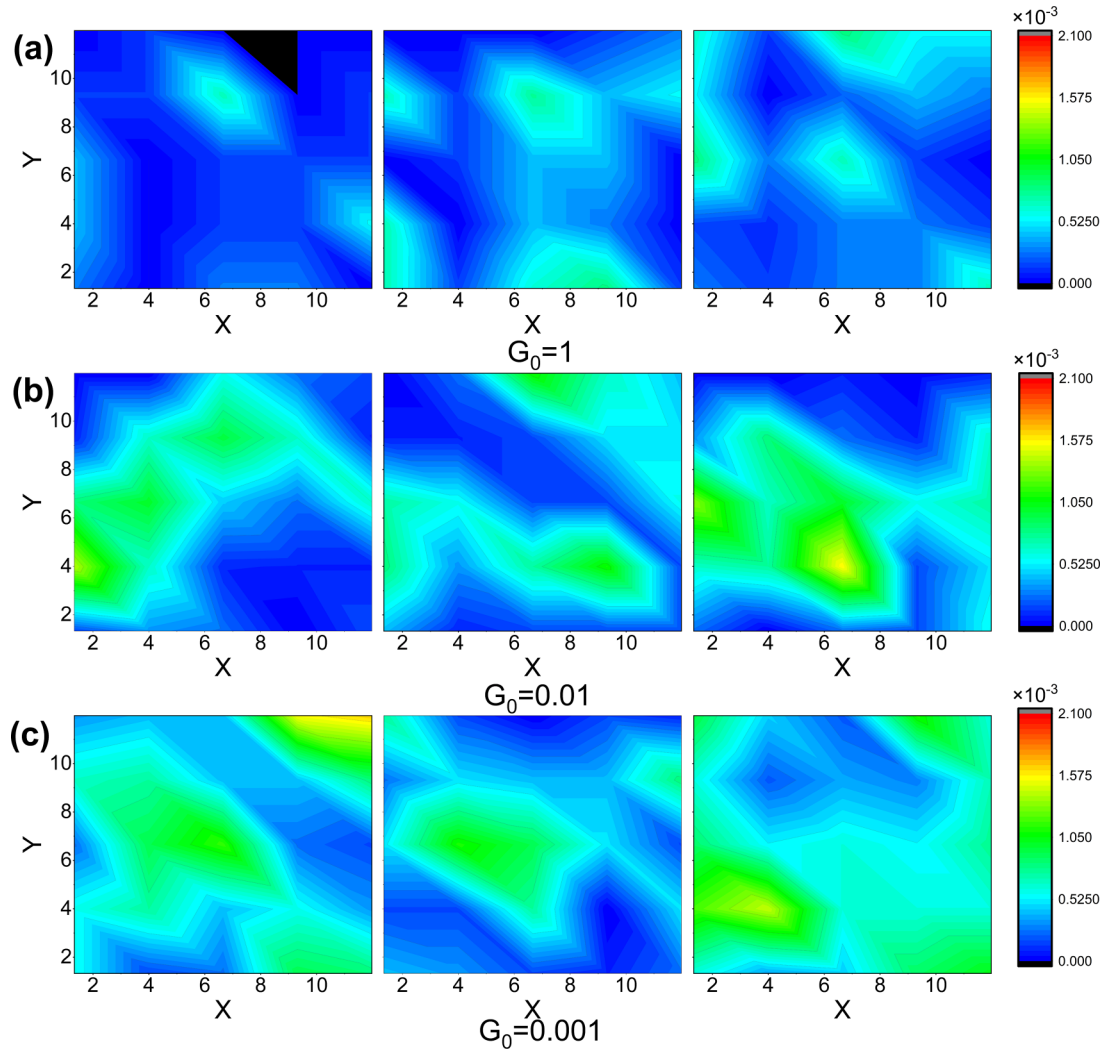

FIG. 8. Probability-density distributions of hopping events for high-fragility and low-fragility systems. (a) $G_0 = 1$, $T = 1.02\ T_g$ (top), (b) $G_0 = 0.01$, $T = 1.02\ T_g$ (middle), and (c) $G_0 = 0.001$, $T = 1.02\ T_g$ (bottom).

significantly enhanced with decreasing G_0 or increasing kinetic fragility. The strong dynamic heterogeneity in fragile liquids means that the hopping facilitation is slowed down on approaching T_g. The persistence time thus rapidly rises, and the coupling between the persistence time and the waiting time associated with successive hops is broken down. Instead, the fractional coupling is held, as demonstrated in Fig. 4(a). Furthermore, reducing exponent values are required in more fragile liquids due to their increasing dynamic heterogeneity. We further compare the probability-density distributions of the system at $G_0 = 0.01$ with that at $G_0 = 0.001$ [Figs. 8(b) and 8(c)], and do not find the distinct difference in size and shape of mobile regions between them. It suggests that the dynamic heterogeneity approaches a maximum corresponding to the lower limit of the fractional SE exponent. This process is accompanied by the divergence of fragility.

To more quantitatively study the dynamic heterogeneity at various G_0, we calculate the dynamic susceptibility, χ_4, which is defined as the long-wavelength limit of dynamic structure factor, $\chi_4(t) = \lim_{\tilde{q}\to 0} S_4(\mathbf{q}, t)$. The dynamic structure factor is given by the four-point correlation function in the Fourier space,

$$S_4(\mathbf{q}, t) = \int e^{i\mathbf{q}\cdot r} G_4(r, t) dr$$

$$= N\left\langle \left| \frac{1}{N} \sum_j e^{i\mathbf{q}\cdot r_j(0)} (c_j(t, 0) - F_s(\mathbf{q}, t)) \right|^2 \right\rangle, \quad (5)$$

where the overlap function is $c_j(t, 0) = e^{i\mathbf{q}\cdot[r_j(t) - r_j(0)]}$. Figures 9(a) and 9(b) plot $\chi_4(t)$ at various temperatures for $G_0 = 1$ and 0.001. The dynamic heterogeneity is shown to be enhanced by decreasing temperature, and moreover, the enhancement is more pronounced in high-fragility liquids on approaching T_g [Fig. 9(b)]. We compare the maxima of χ_4, $\chi_{4\max}$ as a function of structural relaxation time at $G_0 = 1$, 0.1, 0.01, and 0.001, as shown in Fig. 9(c), which further clarifies the relation between dynamic heterogeneity and fragility. Corresponding to the results shown in Figs. 9(a) and 9(b), a little difference in dynamic heterogeneity measured by $\chi_{4\max}$ is found at relatively high temperatures, but it becomes quite significant at temperatures close to T_g. As per our common

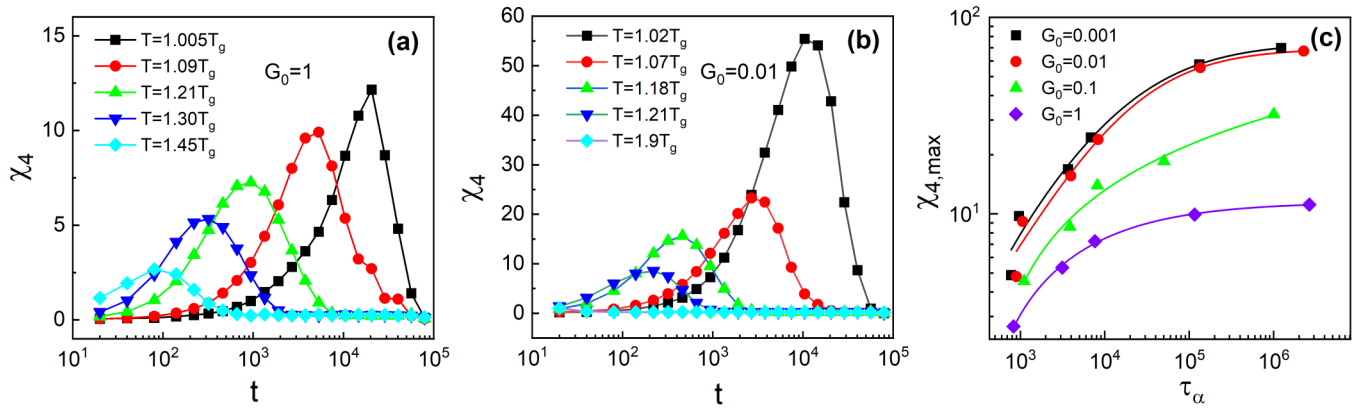

FIG. 9. Dynamic susceptibility $\chi_4(t)$ of DPGM systems. (a)$\chi_4(t)$ of low-fragility system ($G_0 = 1$) at different temperatures above T_g. (b) $\chi_4(t)$ of high-fragility system ($G_0 = 0.01$) at different temperatures above T_g. (c)$\chi_{4,\max}$ as function of structural relaxation time, τ_α at $G_0 = 1$, 0.1, 0.01, and 0.001. Solid lines are guide for eyes.

knowledge, the more fragile the liquids, the more heterogeneous they are. However, for these very fragile liquids that even exceed the available fragility limit in real glassy materials, the difference in $\chi_{4\max}$ is predicted to be quite tiny at a given relaxation time, such as the cases of $G_0 = 0.01$ and 0.001. It suggests that there is no remarkable difference in dynamic heterogeneity among very fragile liquids, or in other words, a possible existence of an upper bound of dynamic heterogeneity in high-fragility regime, which corresponds to the lower bound of decoupling of Stokes-Einstein relation.

We check the experimental data of supercooled liquids in the reported literature [29,49]. The fractional SE exponents of most glass-forming liquids are above the lower limit of 0.540 predicted by this work; in particular, the values for some multicomponent alloys are close to 0.540 [29]. We also note that the exponents for a few phase-change materials above their melting points are much smaller than 0.54, approximately 0.36 for $Ag_4In_3Sb_{67}Te_{26}$ alloy, for example [49]. The abnormally low-exponent systems show the pronounced heterogeneity of chemical stoichiometry due to the impurity doping [49]. Thus, it is possible that these liquids have strong dynamic heterogeneity compared to glass-forming liquids, which will lead to the violation of the SE relation and even very small components of fractional coupling in high-temperature regions. The decoupling limit predicted in this work needs more experimental evidence in a wide variety of glass formers. A primary challenge may come from the difficulty of the measurement of self-diffusion coefficients in highly supercooled region.

IV. CONCLUSIONS

In summary, we propose a distinguishable-particle glassy model that can model the glass-forming liquids with ultrawide-fragility range ($26 \leqslant m_d \leqslant 343$ in this work). Using this model, we examine the fractional SE relation in glass-forming liquids and provide a quantitative relation between the SE exponent and the kinetic fragility. The results predict that the fractional SE exponent is rapidly reduced with increasing kinetic fragility and approaches a lower bound of 0.540 in very fragile liquids. The decoupling of the SE relation as well as its fragility dependence is well interpreted by the hopping dynamics of single particles. This work gives an overall picture of the SE relation in glass family, and meanwhile, DPGM provides us an ideal candidate to study the fragility dependence of glassy properties by means of a simple pair interactive system.

ACKNOWLEDGMENTS

We acknowledge financial support from National Natural Science Foundation of China Grants No. 52031016, No. 52071029, and No. 11974297, and Hong Kong General Research Fund No. 11974297. The computer resources at the Shanghai and Guangzhou Supercomputer Center are gratefully acknowledged.

[1] M. D. Ediger, Spatially heterogeneous dynamics in supercooled liquids, Annu. Rev. Phys. Chem. **51**, 99 (2000).

[2] L. Berthier and G. Biroli, Theoretical perspective on the glass transition and amorphous materials, Rev. Mod. Phys. **83**, 587 (2011).

[3] L. Berthier, G. Biroli Ludovic, J.-P. Bouchaud, L. Cipelletti, and W. van Saarloos, *Dynamical Heterogeneities in Glasses, Colloids, and Granular Media* (Oxford University Press, Oxford, 2011).

[4] W. Kob, C. Donati, S. J. Plimpton, P. H. Poole, and S. C. Glotzer, Dynamical Heterogeneities in a Supercooled Lennard-Jones Liquid, Phys. Rev. Lett. **79**, 2827 (1997).

[5] H. B. Yu, W. H. Wang, and K. Samwer, The β relaxation in metallic glasses: An overview, Mater. Today **16**, 183 (2013).

[6] P. Luo, P. Wen, H.Y. Bai, B. Ruta, and W. H. Wang, Relaxation Decoupling in Metallic Glasses at Low Temperatures, Phys. Rev. Lett. **118**, 225901 (2017).

[7] H. B. Yu, R. Richert, and K. Samwer, Structural rearrangements governing Johari-Goldstein relaxations in metallic glasses, Sci. Adv. **3**, e1701577 (2017).

[8] G. Tarjus and D. Kivelson, Breakdown of the Stokes–Einstein relation in supercooled liquids, J. Chem. Phys. **103**, 3071 (1995).

[9] X. Monnier, D. Cangialosi, B. Ruta, R. Busch, and I. Gallino, Vitrification decoupling from β-relaxation in a metallic glass, Sci. Adv. **6**, eaay1454 (2020).

[10] K. R. Harris, The fractional Stokes–Einstein equation: Application to Lennard-Jones, molecular, and ionic liquids, J. Chem. Phys. **131**, 054503 (2009).

[11] S. R. Becker, P. H. Poole, and F. W. Starr, Fractional Stokes-Einstein and Debye-Stokes-Einstein Relations in a Network-Forming Liquid, Phys. Rev. Lett. **97**, 055901 (2006).

[12] C. A. Angell, Relaxation in liquids, polymers and plastic crystals - strong/fragile patterns and problems, J. Non-Cryst. Solids **131**, 13 (1991).

[13] C. A. Angell, Formation of glasses from liquids and biopolymers, Science **267**, 1924 (1995).

[14] P. G. Debenedetti and F. H. Stillinger, Supercooled liquids and the glass transition, Nature (London) **410**, 259 (2001).

[15] J. Horbach, W. Kob, and K. Binder, The dynamics of supercooled silica: Acoustic modes and boson peak, Philos. Mag. B **235**, 320 (1998).

[16] D. Richter, B. Frick, and B. Farago, Neutron-spin-echo Investigation on the Dynamics of Polybutadiene near the Glass Transition, Phys. Rev. Lett. **61**, 2465 (1988).

[17] T. Scopigno, G. Ruocco, F. Sette, and G. Monaco, Is the fragility of a liquid embedded in the properties of its glass? Science **302**, 849 (2003).

[18] J. Geske, B. Drossel, and M. Vogel, Fragile-to-strong transition in liquid silica, AIP Adv. **6**, 035131 (2016).

[19] K. N. Lad, N. Jakse, and A. Pasturel, Signatures of fragile-to-strong transition in a binary metallic glass-forming liquid, J. Chem. Phys. **136**, 104509 (2012).

[20] L. H. Zhang and C. H. Lam, Emergent facilitation behavior in a distinguishable-particle lattice model of glass, Phys. Rev. B **95**, 184202 (2017).

[21] C. S. Lee, M. Lulli, L. H. Zhang, H. Y. Deng, and C. H. Lam, Fragile Glasses Associated with a Dramatic Drop of Entropy under Supercooling, Phys. Rev. Lett. **125**, 265703 (2020).

[22] L. S. Shagolsem, D. Osmanović, O. Peleg, and Y. Rabin, Communication: Pair interaction ordering in fluids with random interactions, J. Chem. Phys. **142**, 051104 (2015).

[23] W. Kob and H. C. Andersen, Testing made-coupling theory for a supercooled binary Lennard-Jones mixture: The van Hove correlation function, Phys. Rev. E **51**, 4626 (1995).

[24] See Supplemental Material at http://link.aps.org/supplemental/10.1103/PhysRevB.108.104105 for the technical details about the single-particle dynamics, the simulation results on the mean-squared displacements and radial distribution functions at different kinetic fragility.

[25] I. Echeverria, P. C. Su, S. L. Simon, and D. J. Plazek, Physical aging of a polyetherimide: Creep and DSC measurements, J. Polym. Sci., Part B: Polym. Phys. **33**, 2457 (1995).

[26] L. M. Wang, C. A. Angell, and R. Richert, Fragility and thermodynamics in nonpolymeric glass-forming liquids, J. Chem. Phys. **125**, 074505 (2006).

[27] R. Böhmer, K. L. Ngai, C. A. Angell, and D. J. Plazek, Nonexponential relaxations in strong and fragile glass formers, J. Chem. Phys. **99**, 4201 (1993).

[28] G. L. Pollack, Atomic test of the Stokes-Einstein law: Diffusion and solubility of Xe, Phys. Rev. A **23**, 2660 (1981).

[29] J. F. Douglas and D. Leporini, Obstruction model of the fractional Stokes–Einstein relation in glass-forming liquids, J. Non-Cryst. Solids **235**, 137 (1998).

[30] C. T. Moynihan and C. A. Angell, Bond lattice or excitation model analysis of the configurational entropy of molecular liquids, J. Non-Cryst. Solids **274**, 131 (2000).

[31] K. Vollmayr-Lee, W. Kob, K. Binder, and A. Zippelius, Dynamical heterogeneities below the glass transition, J. Chem. Phys. **116**, 5158(2002).

[32] S. G. M. Razul, G. S. Matharoo, and P. H. Poole, Spatial correlation of the dynamic propensity in a glass-forming liquid, J. Phys.: Condens. Matter **23**, 235103 (2011).

[33] R. Pastore, A. Coniglio, and M. P. Ciamarra, From cage-jump motion to macroscopic diffusion in supercooled liquids, Soft Matter **10**, 5724 (2014).

[34] Y. J. Lü and W. H. Wang, Single-particle dynamics near the glass transition of a metallic glass, Phys. Rev. E **94**, 062611 (2016).

[35] J. Helfferich, F. Ziebert, S. Frey, H. Meyer, J. Farago, A. Blumen, and J. Baschnagel, Continuous-time random-walk approach to supercooled liquids. I. Different definitions of particle jumps and their consequences, Phys. Rev. E **89**, 042603 (2014).

[36] M. P. Ciamarra, R. Pastore, and A. Coniglio, Particle jumps in structural glasses, Soft Matter **12**, 358 (2016).

[37] C. H. Lam, Repetition and pair-interaction of string-like hopping motions in glassy polymers, J. Chem. Phys. **146**, 244906 (2017).

[38] L. Berthier, D. Chandler, and J. P. Garrahan, Length scale for the onset of Fickian diffusion in supercooled liquids, Europhys. Lett. **69**, 320 (2004).

[39] L. Hedges, L. Maibaum, D. Chandler, and J. P. Garrahan, Decoupling of exchange and persistence times in atomistic models of glass formers, J. Chem. Phys. **127**, 211101 (2007).

[40] L. Larini, A. Ottochian, C. de Michele, and D. Leporini, Universal scaling between structural relaxation and vibrational dynamics in glass-forming liquids and polymers, Nat. Phys. **4**, 42 (2008).

[41] C.-T. Yip, M. Isobe, C. H. Chan, S. Ren, K. P. Wong, Q. Huo, C. S. Lee, Y. H. Tsang, Y. Han, and C. H. Lam, Direct Evidence of Void-Induced Structural Relaxations in Colloidal Glass Formers, Phys. Rev. Lett. **125**, 258001 (2020).

[42] D. Chandler and J. P. Garrahan, Dynamics on the way to forming glass: Bubbles in space-time, Annu. Rev. Phys. Chem. **61**, 191 (2010).

[43] J. P. Garrahan and D. Chandler, Geometrical Explanation and Scaling of Dynamical Heterogeneities in Glass Forming Systems, Phys. Rev. Lett. **89**, 035704 (2002).

[44] G. Adam and J. H. Gibbs, On the temperature dependence of cooperative relaxation properties in glass-forming liquids, J. Chem. Phys. **43**, 139 (1965).

[45] Y. J. Lü, H. R. Qin, and C. C. Guo, Vortex structure of excitation fields in a supercooled glass-forming liquid and its relationship with relaxations, Phys. Rev. B **104**, 224103 (2021).

[46] H. Zhang, C. Zhong, J. F. Douglas, X. Wang, Q. Cao, D. Zhang, and J. Z. Jiang, Role of string-like collective atomic motion on diffusion and structural relaxation in glass forming Cu-Zr alloys, J. Chem. Phys. **142**, 164506 (2015).

[47] A. S. Keys, L. O. Hedges, J. P. Garrahan, S. C. Glotzer, and D. Chandler, Excitations Are Localized and Relaxation is Hierarchical in Glass-Forming Liquids, Phys. Rev. X **1**, 021013 (2011).

[48] C. H. Lam, Local random configuration-tree theory for string repetition and facilitated dynamics of glass, J. Stat. Mech. (2018) 023301.

[49] S. Wei, C. Persch, M. Stolpe, Z. Evenson, G. Coleman, P. Lucas, and M. Wuttig, Violation of the Stokes-Einstein relation in $Ge_2Sb_2Te_5$, GeTe, $Ag_4In_3Sb_{67}Te_{26}$, and $Ge_{15}Sb_{85}$, and its connection to fast crystallization, Acta Mater. **195**, 491 (2020).